Biomass and Bioenergy 99 (2017) 116–121

Contents lists available at ScienceDirect

Biomass and Bioenergy

journal homepage: http://www.elsevier.com/locate/biombioe

Research paper

Kinetic model of cellulose degradation using simultaneous saccharification and fermentation

Kouki Sakimoto, Machi Kanna*, Yukihiko Matsumura

Institute of Engineering, Hiroshima University, 1-4-1 Kagamiyama, Higashi-Hiroshima 739-8527 Japan

ARTICLE INFO

Article history:
Received 23 June 2016
Received in revised form
7 February 2017
Accepted 24 February 2017
Available online 8 March 2017

Keywords:
Cellulose
Simultaneous saccharification and fermentation
Kinetic model
Langmuir adsorption
Michaelis-Menten

ABSTRACT

Numerical analyses of energy production processes are important for practical applications. Here, we established a model of enzymatic hydrolysis and ethanol fermentation. The kinetic model of these reactions were represented by Langmuir adsorption, Michaelis-Menten, and Shuler models. In our model, ethanol fermentation and enzymatic hydrolysis models were fit to experimental data separately, and their model equations were then combined for fitting of experimental data, including the size of cellulose, amount of adsorbed protein, and decreases in glucose as the theoretical production values for SSF. From these kinetic models, the theoretical values for saccharification and fermentation were calculated, and optimal parameters were determined. Using these parameters, theoretical curves for simultaneous saccharification and fermentation were predicted. Additionally, we identified changes in the radius of cellulose and the concentrations of cellulose, cellobiose, glucose, and ethanol during saccharification and fermentation.

1. Introduction

Bioethanol produced from lignocellulosic biomass has potential applications as an alternative to fossil fuels. Lignocellulosic biomass contains three types of polymers, i.e., cellulose, hemicellulose, and lignin. Cellulose, which is the main component of plant cell walls, consists of D-glucose linked by β-1,4 glycoside bonds and has a tightly packed structure owing to strong hydrogen bonding [1]. In contrast, hemicellulose exhibits a complex carbohydrate structure containing multiple types of polymers, which vary among different species. Lignin is a phenylpropanoid polymer containing of p-coumaryl, coniferyl, and sinapyl alcohol. These phenylpropanoids are bound together through various types of linkages [1].

To obtain bioethanol from lignocellulosic biomass, the biomass is subjected to various processes, including pretreatment, enzymatic hydrolysis, and ethanol fermentation. Pretreatment is a deconstruction method involving physical and chemical pulverization. During pretreatment, the accessibility of cellulose is improved [2], and glucose can then be obtained from cellulose through enzymatic hydrolysis. Finally, during the ethanol production step, glucose can be converted to ethanol by fermentation using a variety of microorganisms [3].

In general, enzymatic hydrolysis and ethanol fermentation are performed separately. However, effective ethanol production can be achieved by carrying out enzymatic hydrolysis and ethanol fermentation in same reactor. In this method, enzymatic hydrolysis and fermentation is performed simultaneously (termed simultaneous saccharification and fermentation [SSF]) [4]. SSF is a cost-effective, simple method compared with separate hydrolysis and fermentation (SHF). Moreover, SSF may allow high levels of production owing to reduced end-product inhibition during enzymatic hydrolysis [5]. Therefore, numerous studies have been performed to establish SSF as a feasible method, using biomass (i.e., wood, herbaceous biomass) as the starting material for practical applications.

Numerical analyses based on common reactions are needed in order to evaluate the large amounts of data produced by studies of SSF and to improve the SSF process. In previous studies, empirical models have been established for various analytical purposes [6]. Enzymatic hydrolysis during SSF is complex and requires a variety of enzymes. For example, cellobiohydrolase and end-glucanase hydrolyze cellulose after its adsorption, and cellobiose is generated by cellobiohydrolase and converted to glucose by β-glucosidase. A previous study modeled this enzyme adsorption process using Langmuir adsorption [7–9]. Kadam et al. investigated enzymatic saccharification using the Langmuir model with xylose [7]. In

* Corresponding author. Tel./fax: +81 82 424 2430.
E-mail address: kanna@hiroshima-u.ac.jp (M. Kanna).

http://dx.doi.org/10.1016/j.biombioe.2017.02.016
0961-9534/

another study, Langmuir adsorption was applied to enzymatic hydrolysis and fit well with the experimental result [9]. Thus, inactivation of adsorbed enzyme may cause a delay in the rate of enzymatic hydrolysis. For establishment of a more suitable model, in addition to the inactivation rate, it is also necessary to consider changes in the radius of cellulose over time. Importantly, Langmuir adsorption has also been used for analysis of adsorption of Avicell and biomass [10], and the Michaelis-Menten model has been used for analysis of cellulose degradation [11]. Moreover, Kadam et al. used a combined model involving Langmuir adsorption and the Michaelis-Menten model [7]. This model fit well with the experimental data.

In addition to enzymatic hydrolysis, ethanol fermentation after enzymatic hydrolysis is necessary for ethanol production. Numerical analysis of the rate of ethanol production can provide insights into effective production methods because changes in each substance can be deduced. Additionally, Kumar et al. described a fermentation model that included substrate and product inhibition, cell numbers, and the maintenance coefficient [12]. These factors are likely to be important for establishment of an effective model of cellulose degradation using SSF.

Therefore, in this study, we aimed to establish an SSF model for cellulose degradation based on these previous models. In our model, ethanol fermentation and enzymatic hydrolysis models were fit to experimental data separately, and their model equations were then combined for calculation of experimental data, including the size of cellulose, amount of adsorbed protein, and decreases in glucose as the theoretical production values for SSF. Our numerical analysis demonstrated that these factors could be altered based on the model parameters, providing important insights into the cellulose degradation process.

2. Material and methods

2.1. Enzymatic hydrolysis

Cellulose (Sigma cell type 20; Sigma-Aldrich, Japan) were used for enzymatic saccharification. For quantification of glucose amount after enzymatic hydrolysis, glucose (Wako Pure Chemical Industries, Japan) was used as standard of high performance liquid chromatography. Enzymatic hydrolysis was carried out in a 200-mL Erlenmeyer flask. One gram of cellulose was used as a substrate for enzymatic hydrolysis, and 200 U/g substrate cellulase from *Trichoderma reesei* (Sigma-Aldrich) and 350 U/g substrate β-glucosidase (TOYOBO, Japan) were added to the flask. As enzymatic hydrolysis buffer, we used 0.01 M sodium acetate buffer which was adjusted to pH 5.0 using NaOH. Enzymatic hydrolysis was performed in an incubator with shaking. The incubation temperatures were 30 °C and 40 °C. Samples were collected at 0, 6, 12, 24, 48, and 72 h.

2.2. Ethanol fermentation

Ethanol fermentation was performed in a 200-mL Erlenmeyer flask at constant temperature (30 °C or 40 °C) and pH 5.0. Glucose (1.11 g) was used as the substrate. *Saccharomyces cerevisiae* type II (Sigma-Aldrich Japan) was precultured in YPD solution (10 g/L yeast extract, 20 g/L peptone, and 20 g/L dextrose; Difco BD Japan) at 48 h and adjusted to an OD_{600} of 1 0.0. After dilution of cell culture, 2 mL of the yeast culture was added to the flask. As the fermentation medium, peptone and yeast extract (Wako Chemicals Japan) were used at 20 and 10 g/L, respectively. Samples were collected at 0, 6, 12, 24, and 48 h.

2.3. Analysis

Glucose, cellobiose, and ethanol concentrations were analyzed by high-performance liquid chromatography (Shimadzu, Japan) operated at 60 °C with KS-802 (Shodex Japan). The eluent was deionized water, and the flow rate was 0.7 mL/min.

3. Kinetic analysis

One type of cellulase, endo-glucanase (EG), randomly cleaves internal bonds at amorphous site of cellulose, whereas cellobiohydrolase (CBH) produces cellobiose from the non-reducing terminal of cellulose. Moreover, cellobiose is hydrolyzed to glucose by β-glucosidase. Thus, we defined the reaction schemes for saccharification as cellulose → glucose and cellulose → cellobiose → glucose. Moreover, because cellobiohydrolase and EG adsorb to solid cellulose, these reactions are thought to represent liquid-solid reactions and can be based on the Langmuir adsorption model. On the other hand, glucose and cellobiose generated by hydrolysis are soluble in liquid; because the cellobiose-glucose reaction is a homogeneous reaction, this reaction model was based on the Michaelis-Menten model.

During the fermentation step, glucose is converted to ethanol. The fermentation model used in this study was described by Kumar et al. (2013) [12], and is based on the Monod equation. In SSF, saccharification and fermentation are conducted simultaneously. Therefore, it was necessary to consider the four reactions (two enzymatic hydrolysis reactions using the Langmuir model, one enzymatic reaction using the Michaelis-Menten model, and ethanol fermentation) to obtain the SSF model. Furthermore, because glucose generated by enzymatic hydrolysis is immediately converted to ethanol, glucose inhibition by β-glucosidase can be neglected.

First, because enzymes adsorbed to cellulose, we described the rates of adsorption and desorption as follows:

$$\vec{v} = K[E](N_s - N_a) \tag{1}$$

$$\overleftarrow{v} = K'N_a \tag{2}$$

where [E] is enzyme (M), and Na and Ns are the number of adsorptions and adsorption sites, respectively.

When the adsorption and desorption rates were in equilibrium, the covering rate (N_a/N_s) could be expressed as follows ($K_s = K/K'$).

$$\theta = \frac{N_a}{N_s} = \frac{K_s[E]}{1 + K_s[E]} \tag{3}$$

From Eqs. (1) and (3), the adsorption rate could be represented by Eq. (4) when the maximum adsorption rate was V_{max} ($\theta = 1$):

$$\vec{v} = \frac{dNa}{dt} = V_{max}\frac{K_s[E]}{1 + K_s[E]} \tag{4}$$

The amount of adsorbed enzyme is shown below. [EC] can be represented by Eq. (5);

$$[EC] = 4\pi r^2 K_E N_a N_C \tag{5}$$

where [EC] is the adsorbed enzyme to cellulose concentration (M), r is the radius of cellulose, K_E is a reaction constant, and N_C is the number of cellulose particles. The rate of cellulose hydrolysis can be described using the following two equations:

$$\frac{d[C]}{dt} = -K_C[EC] \tag{6}$$

$$\frac{d[C]}{dt} = 4\pi r^2 \frac{dr}{dt} \rho N_C \tag{7}$$

where [C] is the cellulose concentration (M). From Eqs. (6) and (7), the change in the radius of cellulose can be calculated as follows:

$$\frac{dr}{dt} = -\frac{1}{4\pi r^2 \rho N_C} K_C[EC] \tag{8}$$

Enzyme adsorbed to cellulose occasionally does not react [13]. Furthermore, because cellulose was converted into sugars by enzymatic hydrolysis, we considered the relationships among the product, nonreacted enzyme, and number of cellulose molecules that adsorbed enzyme. Thus, the adsorbed enzyme reaction was expressed as follows:

$$[EC] \rightarrow [S] + [EC]_{no} \tag{9}$$

where [S] is sugars (cellobiose or glucose), $[EC]_{no}$ is adsorbed enzyme to cellulose without reaction. Thus, the increment of $[EC]_{no}$ was calculated as follows:

$$\frac{d[EC]_{no}}{dt} = K_m[EC] \tag{10}$$

The cellulose conversion rate could then be defined as follows:

$$\frac{d[C]}{dt} = -K_C[EC]_{react} \tag{11}$$

$$[EC]_{react} = [EC] - [EC]_{no} \tag{12}$$

where [EC] is the amount of enzyme adsorbed to cellulose. The adsorption rate was described as [Na]; Na1 and Na2 were the adsorption rats of cellobiohydrolase and EG using Langmuir adsorption, as follows:

$$\frac{dNa1}{dt} = V_{1max}\frac{K_{s1}[E]}{1 + K_{s1}[E]} \tag{13}$$

$$\frac{dNa2}{dt} = V_{2max}\frac{K_{s2}[E]}{1 + K_{s2}[E]} \tag{14}$$

Importantly, EC could be used to determine the changes in cellulose amount and size, and E_1C and E_2C represented cellulose degradation by cellobiohydrolase and EG, as follows:

$$[E_1C] = 4\pi r^2 K_{E1} N_{a1} N_C \tag{15}$$

$$[E_2C] = 4\pi r^2 K_{E2} N_{a2} N_C \tag{16}$$

$$\frac{d[E_1C]_{no}}{dt} = K_{m1}[E_1C] \tag{17}$$

$$\frac{d[E_2C]_{no}}{dt} = K_{m2}[E_2C] \tag{18}$$

$$[E_1C]_{react} = [E_1C] - [E_1C]_{no} \tag{19}$$

$$[E_2C]_{react} = [E_2C] - [E_2C]_{no} \tag{20}$$

$$\frac{dr}{dt} = -\frac{1}{4\pi r^2 \rho N_C}\left(K_{C1}[E_1C]_{react} - K_{C2}[E_2C]_{react}\right) \tag{21}$$

$$\frac{d[C]}{dt} = -K_{C1}[E_1C]_{react} - K_{C2}[E_2C]_{react} \tag{22}$$

Cellobiohydrolase produces cellobiose by hydrolysis of cellulose. The amount of cellobiose depends on the hydrolyzed cellulose according to the adsorption reaction,

$$\frac{d[B]}{dt} = K_{C2}[E_2C]_{react} - \frac{V_{3max}[B]}{K_3 + [B]} \tag{23}$$

Although cellobiohydrolases are described in Langmuir adsorption, β-glucosidase hydrolyzes cellobiose to glucose, and this reaction is represented by the Michaelis-Menten model. According to the Michaelis-Menten mechanism, cellobiose [B] binds reversibly with the enzyme [E] to form the enzyme-cellobiose complex [EB] [14]. Then, [EB] proceeds to glucose [G], as shown in Eq. (11).

$$[E] + [B] \leftrightarrow [EB] \rightarrow [E] + [G] \tag{24}$$

Thus, the Michaelis-Menten equation can be written as follows:

$$\frac{d[G]}{dt} = \frac{V_{3max}[B]}{K + [B]} \tag{25}$$

In addition to enzymatic hydrolysis, SSF also involves ethanol fermentation. Cell growth and ethanol production can be determined used the Monod equation. In a previous report, a model was developed using cell mass formation [X], ethanol production [P], and substrate consumption [G] for fermentation, as follows [12]:

$$\frac{d[X]}{dt} = \frac{\mu_m[G]}{K_{SG} + [G]}[X] - K_d[X] \tag{26}$$

$$\frac{d[P]}{dt} = \frac{\nu_m[G]}{K_{SP} + [G]}[X] \tag{27}$$

$$\frac{d[G]}{dt} = -\frac{1}{Y'_{P/G}}\left(\frac{d[P]}{dt}\right) - \frac{1}{Y'_{X/G}}\left(\frac{d[X]}{dt}\right) - K_{CM}[X] \tag{28}$$

SSF was carried out through ethanol fermentation by yeast, resulting in production of glucose from cellulose hydrolysis.

$$\frac{d[G]}{dt} = K_{C1}[E_1C]_{react} + \frac{V_{3max}[B]}{K_3 + [B]} - \frac{1}{Y'_{P/G}}\left(\frac{d[P]}{dt}\right) - \frac{1}{Y'_{X/G}}\left(\frac{d[X]}{dt}\right) - K_{CM}[X] \tag{29}$$

$$\frac{d[X]}{dt} = \frac{\mu_m[G]}{K_{SG} + [G]}[X] - K_d[X] \tag{30}$$

$$\frac{d[P]}{dt} = \frac{\nu_m[G]}{K_{SP} + [G]}[X] \tag{31}$$

To validate these model equations, we used the root mean square error (RMSE), which was determined as follows:

$$RMSE = \sqrt{\frac{1}{n}\sum_{i=1}^{n}(\text{Observed values} - \text{Predicted values})^2} \tag{32}$$

4. Results

4.1. Enzymatic hydrolysis

Fig. 1 show changes in the concentration of cellulose, cellobiose, glucose at 30 °C. Cellobiose was not detected for 72 h or during saccharification at 30 °C. Because optimum temperature of enzyme is above 30 °C. We tried to investigate the concentration change of cellulose, cellonbiose, and, glucose at 40 °C (Fig. 3). The saccharification rates of cellulose at 100 h were 40.8% at 30 °C and 48.4% at 40 °C. We calculated the amount of cellulose, cellobiose, and, glucose using model fitting (Figs. 1 and 2, line). Furthermore, we calculated that changes in the concentrations of adsorbed enzyme (i = 1, 2), and the radius of cellulose for saccharification at 30 °C and 40 °C (Figs. 3 and 4). We defined the parameters using this model (Table 1). The each value of RMSE at 30 °C and 40 °C was 0.084 and 0.28 respectively. The adsorption rate of CBH at 40 °C was lower than that at 30 °C (Figs. 2 and 4).

4.2. Ethanol fermentation

Fig. 5 shows the production rates of glucose and ethanol and the concentrations of yeast at 30 °C. At 30 °C, glucose was completely exhausted until 24 h. We calculated each parameters by model fitting (Fig. 5 line). Moreover, we predicted that the change of glucose used for growth and fermentation (Fig. 6). As a result, glucose was consumed both in growth and ethanol production. For fermentation at 40 °C, (Fig. 7), the glucose was not completely consumed. We calculated that the ratio of glucose consumption in growth and fermentation (Fig. 8). The glucose mostly used for fermentation. Table 2 shows the parameters for ethanol fermentation at 30 °C and 40 °C. Each value of the RMSE at 30C and 40C were1.39 and 0.50 respectively.

4.3. SSF simulation

Based on the parameters for saccharification and fermentation, we calculated the theoretical values for SSF using our simulation model. Figs. 9 and 10 show the theoretical cellulose, cellobiose, glucose, ethanol, yeast, and adsorbed enzyme (i = 1, 2) concentrations and the theoretical radius of cellulose during SSF at 30 °C and 40 °C.

5. Discussion

During enzymatic hydrolysis, cellobiose was not obtained because the production rate of cellobiose for the cellulase reaction

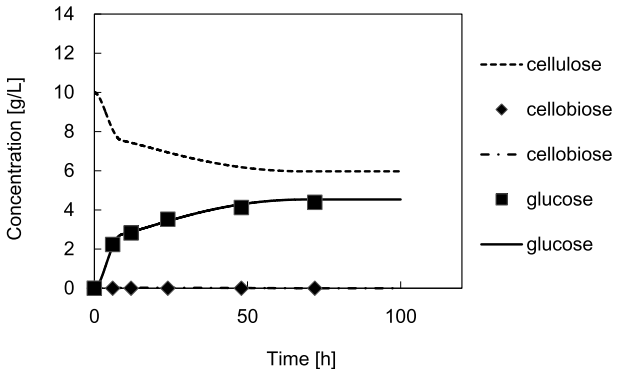

Fig. 1. Curve fitting of cellulose, cellobiose, and glucose concentrations for saccharification at 30 °C.

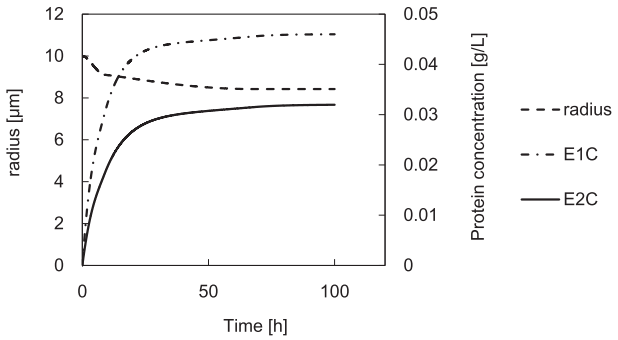

Fig. 2. Simulation results of the radius of cellulose and concentration of adsorbed enzyme (i = 1, 2) for saccharification at 30 °C.

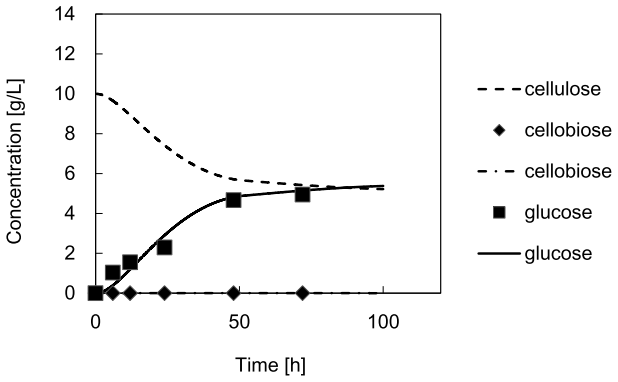

Fig. 3. Curve fitting of cellulose, cellobiose, and glucose concentrations for saccharification at 40 °C.

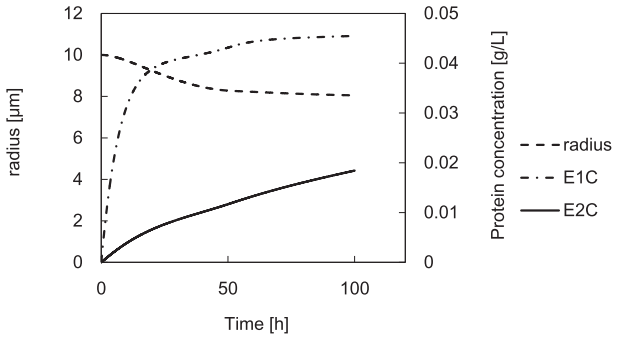

Fig. 4. Simulation results of the radius of cellulose and concentration of adsorbed enzyme (i = 1,2) for saccharification at 40 °C.

Table 1
The parameters for saccharification of cellulose.

	30 °C	40 °C
V_{1max}	6.83×10^{-6}	4.83×10^{-5}
K_{S1}	6.40×10^{-4}	4.70×10^{-3}
K_{E1}	2.90	4.50×10^{-1}
K_{m1}	3.00×10^{-3}	3.90×10^{-3}
k_{C1}	5.60×10^{1}	3.00×10^{-2}
V_{2max}	6.22×10^{-6}	2.90×10^{-6}
K_{S2}	4.50×10^{-3}	2.00×10^{-2}
K_{E2}	3.54	2.00×10^{-1}
K_{m2}	2.90×10^{-4}	2.40×10^{-4}
K_{C2}	3.40×10^{-2}	3.00×10^{-2}
V_{3max}	1.53	1.89
K_3	2.6×10^{1}	3.2×10^{1}

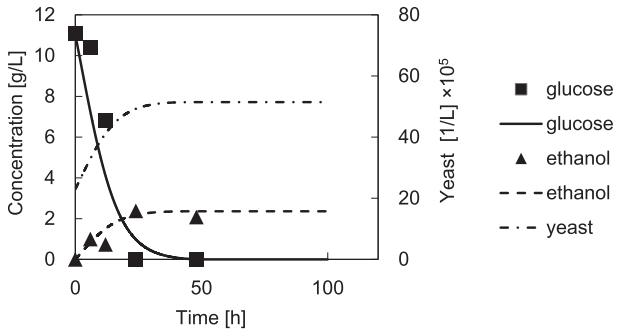

Fig. 5. Curve fitting of glucose, ethanol, and yeast concentrations for saccharification at 30 °C.

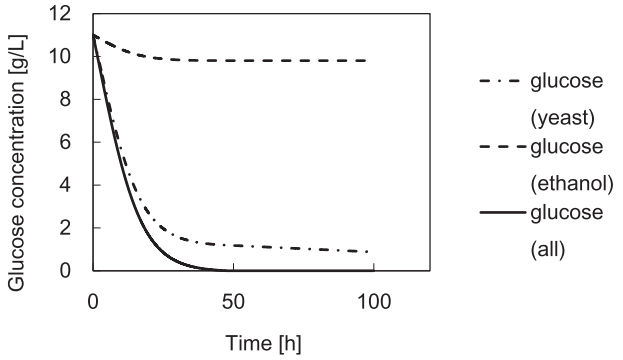

Fig. 6. Simulation results of glucose consumption by yeast growth, ethanol production, and yeast growth plus ethanol production (all) for fermentation at 30 °C.

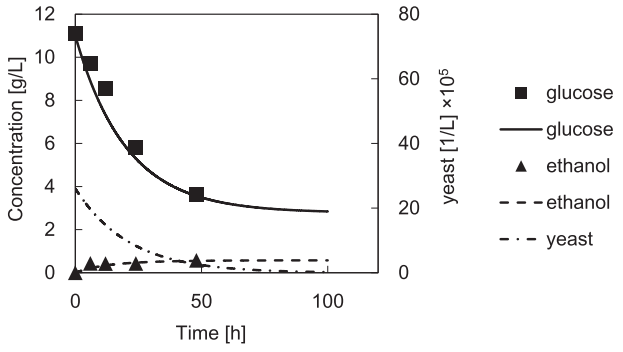

Fig. 7. Curve fitting of glucose, ethanol, and yeast concentrations for fermentation at 40 °C.

(C → B) might be the same as the consumption rate of cellobiose for the β-glucosidase reaction (B → G) (Figs. 1 and 3). Moreover, at 30 °C, the amount of [E_1C] and [E_2C] were higher compared with the amounts of 40 °C. We suggested that many adsorbed enzyme at 30 °C does not hydrolyzed and keep on attaching.

In the fermentation, the yeast concentration was decreased at 40 °C. Because the optimum temperature for *S. cerevisiae* is 30 °C, 40 °C was too high for efficient growth of *S. cerevisiae*(Figs. 5 and 7). The final ethanol concentration at 100 h was 0.58 g/L (conversion rate: 10.3%, Fig. 7). Although glucose mostly used for fermentation at 30 °C, almost all glucose consumption could be attributed to yeast growth at 40 °C (Fig. 8). As mentioned above, because 40 °C is too high for yeast, almost all glucose used for maintenance of yeast itself.

In SSF, the glucose concentration was increased until 8 h at 30 °C

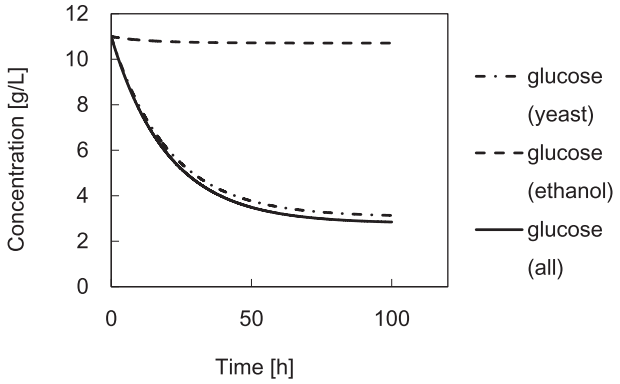

Fig. 8. Simulation results of glucose consumption by yeast growth, ethanol production, and yeast growth plus ethanol production (all) for fermentation at 40 °C.

Table 2
The parameters for ethanol fermentation.

	30 °C	40 °C
μ_m	1.00×10^{-1}	9.46×10^{-3}
K_{SG}	8.96×10^{2}	2.57×10^{3}
K_d	3.48×10^{-8}	8.18×10^{-4}
ν_m	3.29×10^{-2}	1.47×10^{-2}
K_{SP}	3.57×10^{3}	5.70×10^{3}
$Y'_{X/G}$	2.98	2.47
$Y'_{P/G}$	1.98	1.98
K_{CM}	1.98×10^{-6}	5.64×10^{-4}

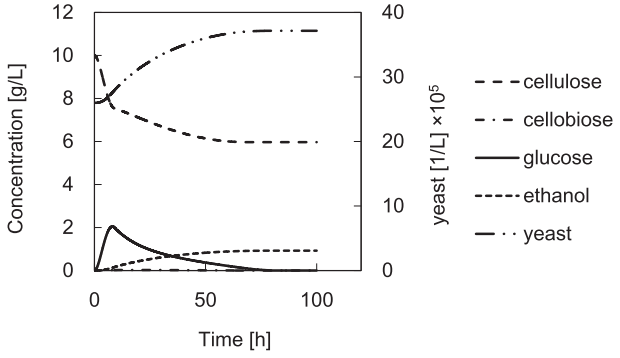

Fig. 9. Calculation results of cellulose, cellobiose, glucose, ethanol, and yeast concentrations over time for SSF at 30 °C.

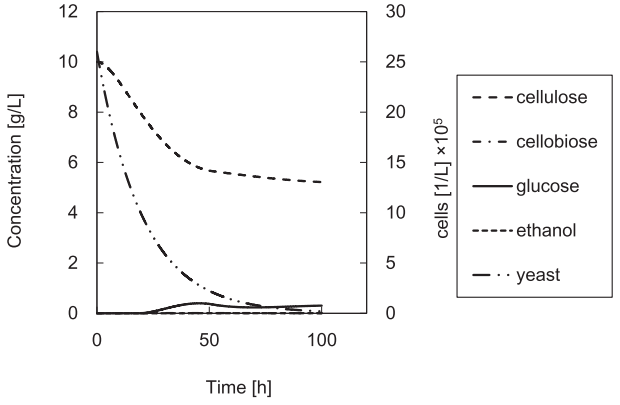

Fig. 10. Calculation results of cellulose, cellobiose, glucose, ethanol, and yeast concentrations over time for SSF at 40 °C.

and then decreased thereafter (Fig. 9). At the beginning of SSF, the amount of glucose was sufficient for ethanol fermentation by yeast. However, the yeast propagated gradually through consumption of glucose. After that, the propagated yeast used glucose for growth and fermentation. Thus, after 8 h, the amount of ethanol began to increase (Fig. 9).

In the simulation results of SSF at 40 °C, although glucose was lower than that at 30 °C, the rate of degradation of cellulose was higher than that at 30 °C. Because optimum temperature of enzymes is more than 40 °C, enzyme activation at 40 °C was higher than that at 30 °C. Therefore, the decomposition rate of cellulose at 40 °C was higher than that at 30 °C. However, the amount of glucose at 40 °C was lower than that at 30 °C. This is because the generated glucose by enzymatic hydrolysis might be used for maintenance for yeast itself. Furthermore, ethanol concentration at 40 °C was extremely low. We believe this result can be explained by the lack of yeast growth at 40 °C, as described above, and the produced glucose at this temperature would be consumed immediately for cell maintenance. The theoretical calculation showed that 11.1 g/L glucose should be converted to 5.62 g/L ethanol. However, the ethanol production at 100 h was only 2.36 g/L, and most of the glucose was consumed for yeast growth (Fig. 8). Accordingly, SSF should be performed at less than 40 °C. In this study, we calculated the amount of glucose, cellobiose, and cellulose by using model fitting. This fitting was performed that ethanol fermentation and enzymatic hydrolysis models were fit to experimental data separately and combined these models. In this study, we suggested that complex reaction such a SSF can be calculated by each individual reaction.

6. Conclusion

In this study, we established a model equation for saccharification and ethanol fermentation. The parameters of saccharification and fermentation were determined by fitting to experimental data, and theoretical values for SSF were calculated using model equations with the determined parameters. From the simulation results, ethanol was not produced at 40 °C. Thus, optimization of SSF should be conducted at less than 40 °C. In this study, we suggested that complicated reaction such a SSF can be calculated by each individual reaction.

Acknowledgement

This work was partly supported by Grants-in-Aid for Scientific Research (KAKENHI) from the Japanese Society for the Promotion of Science (JSPS) (Grant No. 25249142).

References

[1] S.P.S. Chundawat, G.T. Beckham, M.E. Himmel, B.E. Dale, Deconstruction of lignocellulosic biomass to fuels and chemicals, Annu. Rev. Chem. Biomol. Eng. 2 (2011) 121–145.
[2] A.T.W.M. Hendriks, G. Zeeman, Pretreatments to enhance the digestibility of lignocellulosic biomass, Bioresour. Technol. 100 (2009) 10–18.
[3] J.R. Mielenz, Ethanol production from biomass: technology and commercialization status, Curr. Opin. Microbiol. 4 (2001) 324–329.
[4] M. Takagi, S. Abe, S. Suzuki, G.H. Emert, N. Yata, A method for production of alcohol directly from cellulose using cellulase and yeast, in: T.K. Ghose (Ed.), Proceedings Bioconversion Symposium, IIT, New Delhi, 1977, pp. 551–571.
[5] K. Olofsson, M. Bertilsson, G. Lidén, A short review on SSF – an interesting process option for ethanol production from lignocellulosic feedstocks, Biotechnol. Biofuels 1 (2008) 7.
[6] P. Bansal, M. Hall, M.J. Realff, J.H. Lee, A.S. Bommarius, Modeling cellulase kinetics on lignocellosic substrates, Biotechnol. Adv. 27 (2009) 833–848.
[7] K.L. Kadam, E.C. Rydholm, J.D. McMillan, Development and validation of a kinetic model for enzymatic saccharification of lignocellulosic biomass, Biotechnol. Prog. 20 (2004) 698–705.
[8] L. Ma, C. Li, Z. Yang, W. Jia, D. Zhang, S. Chen, Kinetics studies on batch cultivation of *Trichoderma reesei* and application to enhance cellulase production by fed-batch fermentation, J. Biotechnol. 166 (2013) 192–197.
[9] Z. Ye, R.E. Berson, Kinetic modeling of cellulose hydrolysis with first order inactivation of adsorbed cellulase, Bioresour. Technol. 102 (2011) 1194–1199.
[10] D.L. Machado, J.M. Neto, J.G.C. Pradella, A. Bonomi, S.C. Rabelo, A.C. Costa, Adsorption characteristics of cellulase and β-glucosidase on Avicel, pretreated sugarcane, bagasse and lignin, Biotechnol. Appl. Biochem. 62 (2015) 681–689.
[11] R.M.F. Bezzera, A.A. Dias, Enzymatic kinetic of cellulose hydrolysis, Appl. Biochem. Biotechnol. 126 (2005) 49–59.
[12] S. Kumar, P. Dheeran, A.P. Singh, I.M. Mishra, D.K. Adhikari, Kinetic studies of ethanol fermentation using Kluyveromyces sp. IIPE453, J. Chem. Technol. Biotechnol. 88 (2013) 1874–1884.
[13] S.A. Maurer, C.N. Bedbrook, C.J. Radke, Cellulase adsorption and reactivity on a cellulose surface from flow ellipsometry, Ind. Eng. Chem. Res. 51 (2012) 11389–11400.
[14] B.P. English, A.M.V. Oijen, W. Min, K.T. Lee, G. Luo, H. Sun, B.J. Cherayil, S.C. Kou, X.S. Xie, Ever-fluctuating single enzyme molecules: Michaelis-Menten equation revisited, Nat. Chem. Biol. 2 (2006) 87–94.